Nauplius
The Journal of The Brazilian Crustacean Society

e-ISSN 2358-2936
www.scielo.br/nau
www.crustacea.org.br

Original Article

A new freshwater crayfish species of *Parastacus* Huxley, 1879 (Malacostraca: Decapoda: Parastacidae) from southern Brazil

Augusto Frederico Huber[1]
Paula Beatriz de Araujo[2]
Felipe Bezerra Ribeiro[2,3]

1 University of Missouri, School of Natural Resources, Fisheries and Wildlife Sciences Program. Columbia, Missouri, United States of America.
AFH E-mail: afh79r@missouri.edu

2 Universidade Federal do Rio Grande do Sul, Programa de Pós-graduação em Biologia Animal, Laboratório de Carcinologia. Porto Alegre, Rio Grande do Sul, Brazil.
PBA E-mail: pabearaujo@gmail.com

3 Universidade de São Paulo, Faculdade de Filosofia, Ciências e Letras de Ribeirão Preto, Laboratório de Biologia Integrativa de Crustáceos. Ribeirão Preto, São Paulo, Brazil.
FBR E-mail: fbribeiro.bio@gmail.com

ZOOBANK: http://zoobank.org/urn:lsid:zoobank.org:pub:D73CB1C7-AB83-4D4B-B654-AAB1A8E67888

ABSTRACT

The present paper describes a new species of freshwater crayfish of the genus *Parastacus* Huxley, 1879 from the municipality of Amaral Ferrador in the state of Rio Grande do Sul, southern Brazil, evaluates its conservation status according to the IUCN Red List Criteria (sub-criterion B1), and updates the identification key for the genus. *Parastacus longidactylus* sp. n. differs from all analyzed species by the large eyes, the prominent and wide rostral carinae, surpassing the rostral basis and extending to the proximal third of the postorbital carinae, postorbital carinae and rostral carinae prominent and with similar lengths, chelipeds carpus dorsomedial surface not divided longitudinally by groove and long dactylus, surpassing the fixed finger. The possible extent of occurrence was estimated to be 6,968 km^2 and the species was recorded in only one location in the Camaquã River basin. The main threats to the region are the replacement of native vegetation by crops and livestock, water pollution and soil erosion. However, because there is only one known location where *Parastacus longidactylus* sp. n. occurs we suggest classifying the species as Data Deficient.

KEYWORDS

Conservation, crustaceans, Parastacoidea, Rio Grande do Sul, taxonomy.

Corresponding Author
Augusto Frederico Huber
afh79r@missouri.edu

Submitted 12 January 2023
Accepted 01 August 2023
Published 19 January 2024

DOI 10.1590/2358-2936e20230496

INTRODUCTION

Freshwater crayfish are conspicuous members of limnetic ecosystems around the world, except in continental Africa and Antarctica (Crandall and Buhay, 2008; Rogers *et al.*, 2020). In South America, 22 species are recorded in the genera *Parastacus* Huxley, 1879 (17 species), *Samastacus* Riek, 1971 (one species), and *Virilastacus* Hobbs, 1991 (four species) (Huber *et al.*, 2020; 2022; Ribeiro *et al.*, 2020; Rudolph, 2015). The former genus is distributed along streams, wetlands, and swamp forests of Brazil, Uruguay, Argentina, and Chile (Ribeiro *et al.*, 2020; De los Rios-Escalante *et al.*, 2022).

Eight new species of *Parastacus* were discovered and described from 2016 to 2022 (Ribeiro *et al.*, 2016; 2017; Huber *et al.*, 2018; 2020; 2022) and its richness is still underestimated. The development of research concerning native South American crayfish is relevant. Firstly, due to the ancient origin of the group, around 85 Ma during the Cretaceous (Toon *et al.*, 2010) and additionally, the South American parastacids, especially *Parastacus,* exhibit peculiar biological characteristics, such as specialized burrowing behavior, intersexuality, and hermaphroditism (Rudolph and Almeida, 2000; Ribeiro *et al.*, 2020).

The state of knowledge of the group, despite the recent advances, is still quite precarious, which has implications for several issues, especially the conservation of the group. Thus, the aim of this paper is to describe a new species of *Parastacus,* endemic to the state of Rio Grande do Sul, southern Brazil, and to assess its conservation status based on the IUCN Red List Criteria. In addition, we update the identification key for the genus.

MATERIAL AND METHODS

The examined material was collected in the municipality of Amaral Ferrador, state of Rio Grande do Sul, southern Brazil. Specimens were illustrated with the aid of a stereomicroscope fitted with a camera lucida. Illustrations were improved with the aid of Nanking ink and tracing paper, then scanned and edited in Photoshop CS6. All measurements were performed with vernier calipers with 0.1 mm accuracy and a millimetric ocular lens on a stereomicroscope. Morphological descriptions follow Ribeiro *et al.* (2016) and setae classification follows Horn *et al.* (2008). Sex was identified based on the morphology of the gonopores, according to Rudolph (1997). The taxonomic classification follows Rogers *et al.* (2020) and the branchial count follows Huxley (1879). The type material is deposited in the Museu de Zoologia da Universidade de São Paulo (MZUSP), São Paulo, Brazil. Other material examined are deposited in the crustacean collections of the Museu Nacional/Universidade Federal do Rio de Janeiro, Rio de Janeiro (MNRJ) and Universidade Federal do Rio Grande do Sul, Porto Alegre (UFRGS).

The extinction risk for the new species was evaluated according to the B1 sub-criterion of the International Union for Conservation of Nature - IUCN (IUCN 2019). For aquatic invertebrates, this sub-criterion takes into consideration the estimated Extent of Occurrence (EOO), calculated based on the hydrographic basins according to the Otto Bacias shape method (level 5) (ANA, 2007) in QGIS 3.10.3 (QGIS Development Team, 2021).

Abbreviations used are:
AreL = Areola Length
AreW = Areola Width
ASL = Antennal Scale Length
ASW = Antennal Scale Width
CD = Carapace Depth
CeL = Cephalon Length
CL = Carapace Length
CMW = Cornea Maximum Width
CW = Carapace Width
FW = Frontal Width
OW = Orbital Width
PL = Pleon Length
POCL = Post Orbital Carina Length
PW = Pleon Width
RCL = Rostral Carina Length
RDL/LDL = Right/Left Dactylus Length
RL = Rostral Length
RML/LML = Right/Left Merus Length
RPrL/LPrL = Right/Left Propodus Length
RPrT/LPrT = Right/Left Propodus Thickness
RPrW/LPrW = Right/Left Propodus Width
RW = Rostral Width
S1 = Pleonal Somite 1

S2 = Pleonal Somite 2
SLP = Thoracic Sternite Lateral Processes
TeL = Telson Length
TeW = Telson Width
TL = Total Length

The definition of each measurement can be found in Ribeiro *et al.* (2016). Additionally, in this contribution, we determine the proportions to classify the dactylus size (X = RDL/RPrL or/and X = LDL/LPrL): Long (X ≥ 65%), Medium (65% > X > 57%), and Short (57% ≥ X).

SYSTEMATICS

Infraorder Astacidea Latreille, 1802

Superfamily Parastacoidea Huxley, 1879

Family Parastacidae Huxley, 1879

Genus *Parastacus* Huxley, 1879

***Parastacus longidactylus* sp. nov.**
(Figs. 1–4)
Zoobank: urn:lsid:zoobank.org:act:EED4209E-8A29-4818-8137-98CBAC4805F7

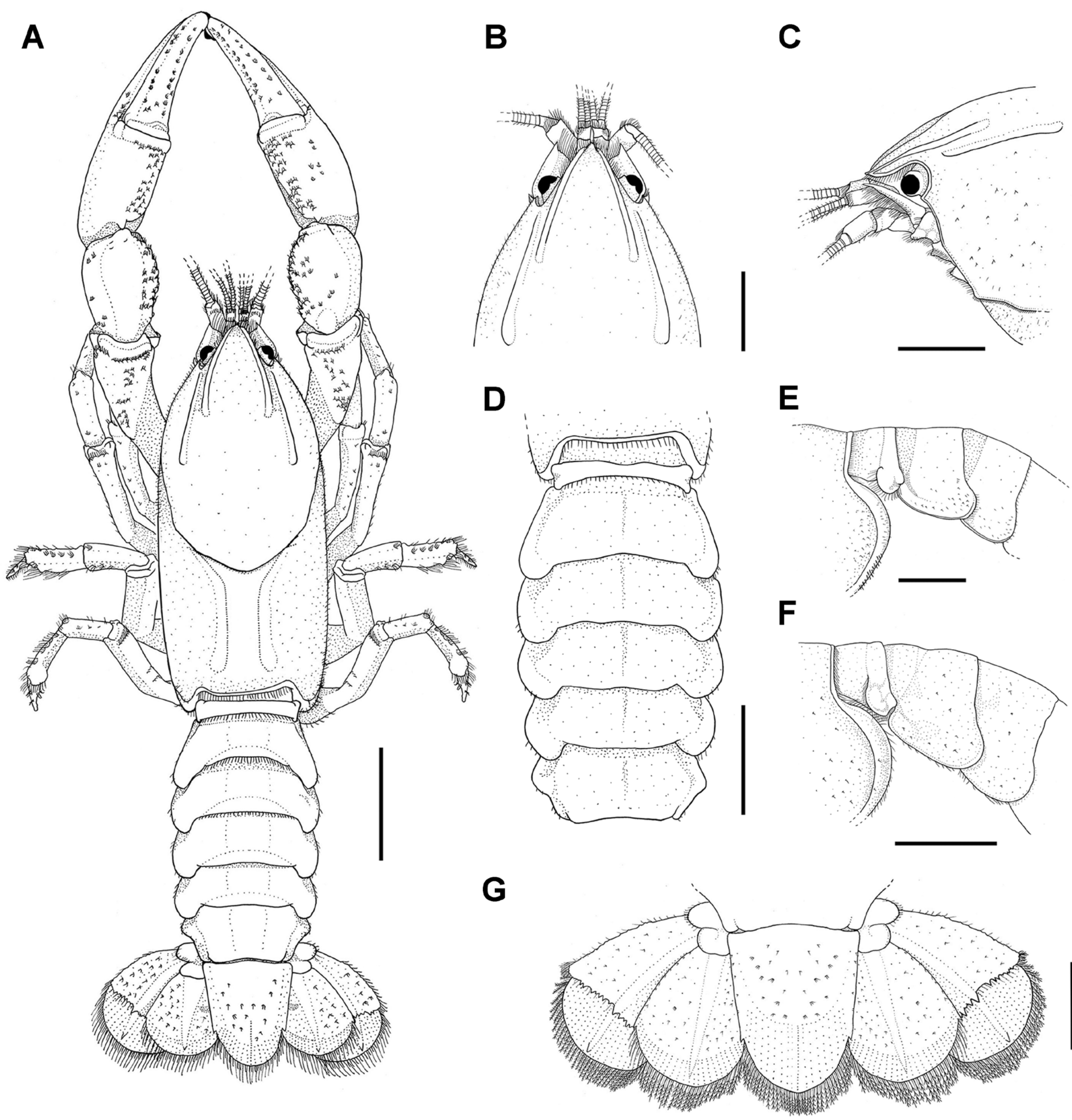

Figure 1. *Parastacus longidactylus* sp. n., holotype (MZUSP 45071) and female paratype (MZUSP 45072) . **A**, Habitus, dorsal view (holotype); **B**, cephalon, dorsal view (holotype); **C**, cephalon, lateral view (holotype); **D**, female abdominal somites, dorsal view (female paratype); **E**, male first, second and third abdominal pleura (holotype); **F**, female first, second and third abdominal pleura (female paratype); **G**, telson and uropods, dorsal view (holotype). Scale bars: **A** = 10 mm; **B**–**F** = 5 mm.

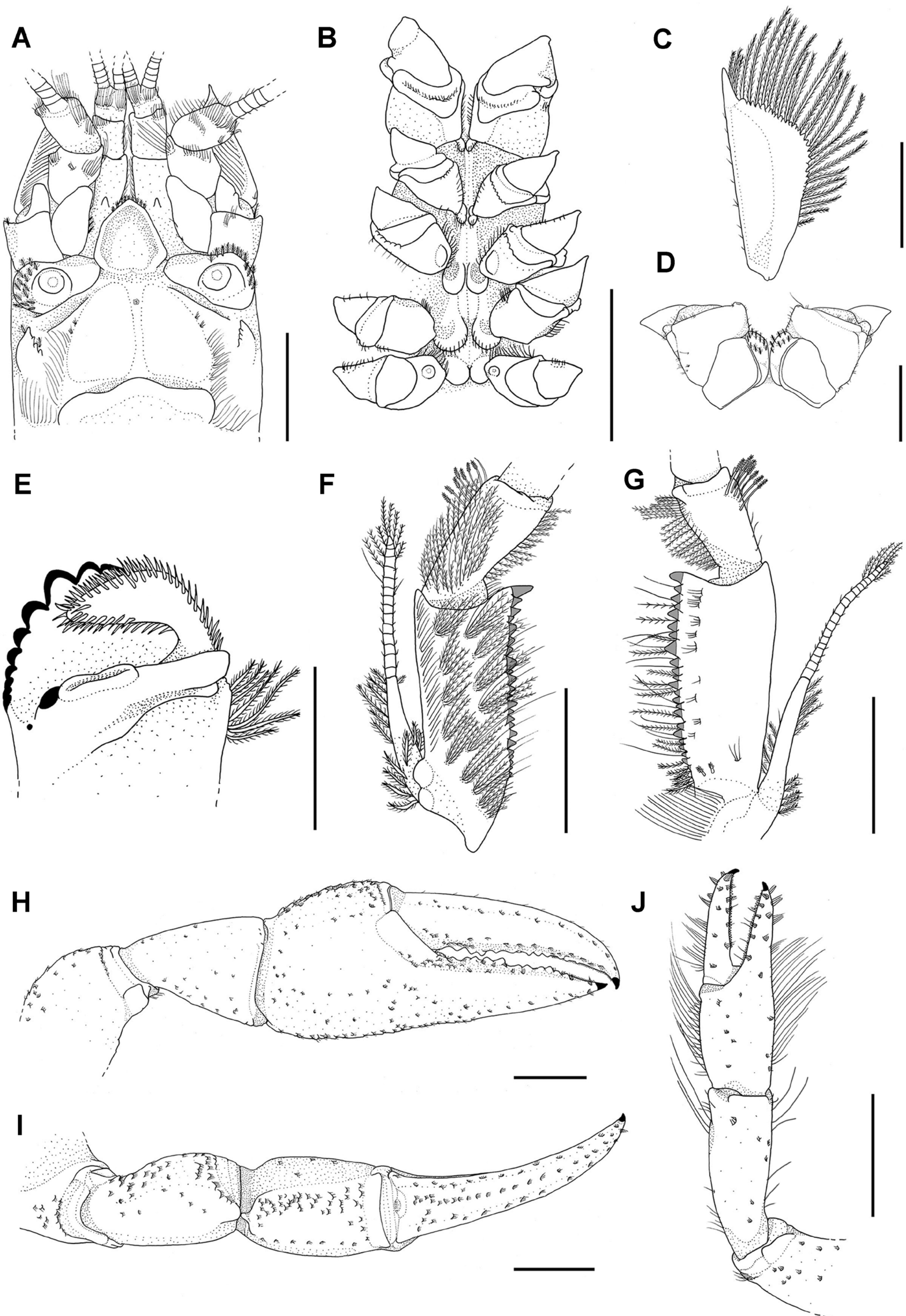

Figure 2. *Parastacus longidactylus* sp. n., holotype (MZUSP 45071) and female paratype (MZUSP 45072). **A**, Epistome (holotype); **B**, thoracic sternites and gonopores (holotype); **C**, thoracomere 8, caudal view (holotype); **D**, antennal scale lateral view (female paratype); **E**, mandible (female paratype); **F**, third maxilliped, ventral view (female paratype); **G**, third maxilliped, dorsal view (female paratype); **H**, first pereiopod, lateral view (holotype); **I**, first pereiopod, dorsal view (holotype); **J**, second pereiopod, lateral view (holotype). Scale bars: **B** = 10 mm; **H**–**J** = 5 mm; **A, F, G** = 3.33 mm; **E** = 2.5 mm; **C** = 2 mm; **D** = 1.5 mm.

Figure 3. *Parastacus longidactylus* sp. n., holotype (MZUSP 45071) in ethanol. **A**, Habitus, dorsal view; **B**, habitus, lateral view. Scale bar = 10 mm.

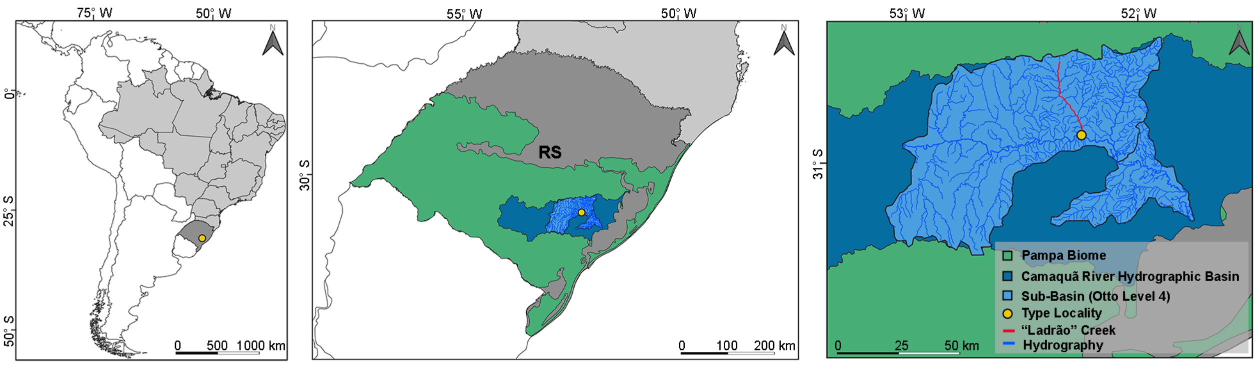

Figure 4. Distribution of *Parastacus longidactylus* sp. n. in Amaral Ferrador, state of Rio Grande do Sul (RS), Brazil.

Type material. Holotype: adult male (MZUSP 45071), Brazil, Rio Grande do Sul, Amaral Ferrador, "Margem do Arroio Ladrão", próximo da junção com o Rio Camaquã (30°52'46.6"S 52°14'33.0"W), VII/2015, coll. unidentified local residents, det. A.F. Huber. Paratypes: 1 female (MZUSP 45072), same data as holotype; 1 male (MZUSP 45073), Brazil, Rio Grande do Sul, Amaral Ferrador, 07/X/2013.

Comparative material. Brazil, Rio Grande do Sul: *Parastacus brasiliensis* (von Martens, 1869): 4 females and 1 male (UFRGS 2337), Mariana Pimentel, 09/X/1986, coll. N.F. Fontoura; 1 female (UFRGS 5757), Porto Alegre, morro Santana, 06/IV/2013, coll. K. M. Gomes; 1 male (UFRGS 5868), sítio do Mato, zona sul, Porto Alegre (30°07'04"S 51°08'47"W), 22/III/2014, coll. M. Pasolius; 2 juveniles and 3 males (UFRGS 5947), Porto Alegre, Parque Natural do Morro do Osso (30°07'07.7"S 51°14'15.1"W), 22/III/2014, coll. K.M. Gomes, F.B. Ribeiro, M.F. Pasolius; 2 juveniles and 3 males (UFRGS 5947), Porto Alegre, Parque Natural do Morro do Osso (30°07'07.7"S 51°14'15.1"W), 22/III/2014, coll. K.M. Gomes, F.B. Ribeiro, M.F. Pasolius; 1 male (UFRGS 6025), rua Dona Francisca, Lomba do Pinheiro, Porto Alegre (30°08'05.0"S 51°06'11.9"W), 26/IX/2014, coll. K.M. Gomes, D.C. Kenne. — *Parastacus buckupi* Huber, Ribeiro and Araujo, 2018: 1 male (UFRGS 3581), Maquiné, arroio Carvão, 25/X/2001, coll. F.S. Vilella; 1 female (UFRGS 3895), Maquiné, arroio Carvão, 25/X/2001, coll. F.S. Vilella. — *Parastacus gomesae* Huber, Araujo and Ribeiro, 2022: 1 male (MNRJ 30203), São Jerônimo, Horto Florestal Quitéria, riacho de primeira ordem (30°29'05.8"S 52°04'09.9"W), 21/X/2020, colls. A.F. Huber, K.M. Gomes, F.B. Ribeiro; 1 female (MNRJ 30204), São Jerônimo, Horto Florestal Quitéria, riacho de primeira ordem (30°29'05.8"S 52°04'09.9"W), 21/X/2020, colls. A.F. Huber, K.M. Gomes, F.B. Ribeiro; 1 female (UFRGS 5339), São Jerônimo (30°29'05.0"S 52°04'11.0"W), VII/2011, colls. K.M. Gomes, C. Sokolowicz. — *Parastacus guapo* Huber, Araujo and Ribeiro, 2022: 1 male (MNRJ 30200), Pantano Grande, Horto Sanga das Pedras, zona alagada (30°13'28.4"S 52°24'44.1"W), 20/X/2020, colls. A.F. Huber; K.M. Gomes, F.B. Ribeiro; 1 female (MNRJ 30201), Pantano Grande, Horto Sanga das Pedras, zona alagada (30°13'28.4"S 52°24'44.1"W), 20/X/2020, colls. A.F. Huber; K.M. Gomes, F.B. Ribeiro; 1 male, 3 females, 2 juveniles (UFRGS 6932), Pantano Grande, Horto Sanga das Pedras, zona alagada (30°13'28.4"S 52°24'44.1"W), 20/x/2020, colls. A.F. Huber; K.M. Gomes, F.B. Ribeiro. — *Parastacus macanudo* Huber, Rockhill, Araujo and Ribeiro, 2020: 1 male (UFRGS 6672), São Leopoldo, Parque Imperatriz Leopoldina (29°45'40.7"S 51°07'47.6"W), 20/VII/2018, colls. A.F. Huber, F.B. Ribeiro; 1 male (MNRJ 29877), São Leopoldo, Parque Imperatriz Leopoldina (29°45'40.7"S 51°07'47.6"W), 20/VII/2018, colls. A.F. Huber, F.B. Ribeiro; 2 males (MNRJ 29877, MNRJ 29878), São Leopoldo, Parque Imperatriz Leopoldina (29°45'40.7"S 51°07'47.6"W), 20/VII/2018, colls. A.F. Huber, F.B. Ribeiro. — *Parastacus promatensis* Fontoura and Conter, 2008: 1 male (UFRGS 4153), São Francisco de Paula, riacho Garapiá, CPCN Pró-Mata (PUCRS), 09/VII/2005, coll. L.C.C. Daudt; 1 female (UFRGS 4157), São

Francisco de Paula, riacho Garapiá, CPCN Pró-Mata (PUCRS), 15/I/2006, coll. L.C.C. Daudt; 1 male (UFRGS 4159), São Francisco de Paula, riacho Garapiá, CPCN Pró-Mata (PUCRS), 09/VII/2005, coll. L.C.C. Daudt; 1 male and 2 females (UFRGS 5949), São Francisco de Paula, riacho Garapiá, CPCN Pró-Mata (29°29'22.0"S 50°13'04.0"W), 2014.

Etymology. A combination of the Latin epithets "longus", which alludes to a long size, and "dactylus", which alludes to fingers. We suggest the common name "the long-finger crayfish" for this new species.

Diagnosis. Wide front with short triangular rostrum. Rostral apex shaped as inverted "U", with straight, blunt spine. Suborbital angle 90°, unarmed. Rostral carinae prominent, wide, surpassing rostral basis, extending to proximal third of postorbital carinae. Postorbital carinae, rostral carinae prominent, with similar length. Cervical groove weakly V-shaped. Areola narrow. Telson subrectangular, longer than wide, with small blunt spines on lateral margins. Mandible with caudal molar process bicuspidate and incisor lobe with 10 teeth. S2 pleurae low and moderate with shallow groove parallel to margin. Chelipeds large and subequal, laterally flattened, with long dactylus surpassing fixed finger. Carpus with dorsomedial surface not divided longitudinally by groove.

Description of the holotype. Rostrum: triangular, wider than long (RL 84.9% of RW), short (11.6% of CL), reaching middle portion of second article of antennular peduncle (Fig. 1A–C). Dorsum straight, apex inverted "U"-shaped, ending in straight blunt spine (Fig. 1A–C). Few plumose setae on lateral margins. Carinae almost straight, prominent, wide, extending back to carapace, surpassing rostral basis, extending to proximal third of postorbital carinae; rostral carinae sides convergent and rostral carinae basis slightly convergent (Fig. 1A–C).

Cephalon: Carapace lacking spines or tubercles. CeL 66.3% of CL. Eyes large (CMW 84.5% of OW); suborbital angle 90°, unarmed (Fig. 1C). Front wide (FW 53.7% of CW). Postorbital carinae and rostral carinae prominent and similar in length (RCL 96.3% of POCL). Lateral cephalic edge with moderate setation (Fig. 1A–C).

Thorax: carapace laterally compressed, deep, narrow (CD 42.4% of CL; CW 35.8% of CL). Cervical groove weakly V-shaped. Branchiocardiac grooves inconspicuous (Fig. 1A). Areola narrow, 3.14× as long as wide (27.7% of CL) (Fig. 1A).

Pleon: lacking spines or tubercles, short, wide (PL 72.9% of CL; PW 98.2% of CW), smooth, covered with small setae on pleural margins (Fig. 1A). Pleural somites with rounded posterior margins. S1 pleurae with large distal lobe not overlapped by S2 pleurae. S2 pleurae low and moderate, with shallow groove parallel to margin (Fig. 1D).

Tailfan: telson more calcified in proximal portion than in distal margin, subrectangular, longer than wide (TeW 80.2% of TeL), with small blunt spines on lateral margins; rounded distal margin with abundant long plumose setae and short simple setae. Dorsal surface with tufts of short setae and inconspicuous dorso-median longitudinal groove (Fig. 1A, E). Uropod protopod bilobed, with rounded and unarmed margins; proximal lobe largest. Exopod lateral margin unarmed, mid-dorsal carinae few prominent, ending in a sharp spine. Transverse suture (diaeresis) straight, with 8 dorsolateral spines (outer) and 8 dorsolateral spines (inner) on right exopod, and 7 dorsolateral spines (outer) and 8 dorsolateral spines (inner) on left exopod. Endopod, mid-dorsal carina weakly projecting, unarmed; lateral margin with 1 sharp spine at level of exopod transverse suture (Fig. 1E).

Epistome: anterolateral section with 4 marginal tubercles on both sides; anterior most tubercle biggest. Posterolateral section with simple setae and with deep lateral grooves converging to basis of anteromedian lobe. Median section with longitudinal groove. Anteromedian lobe irregularly septagonal, 1.04× as long as wide; apex acute, wide, with some small serrated setae, surpassing median part of antepenultimate article of antennal peduncle; apex concave, basis with shallow groove (Fig. 2A).

Thoracic sternites: SLP4 smallest and very close to each other, median keel present and not inflated; SLP5 small and close to each other, median keel present and not inflated; SLP6 larger than SLP4; SLP5 and SLP8 with concave surface, median keel inflated; SLP7 largest, with surface concave, median keel inflated, bullar lobes absent; SLP8 small, median keel absent, vertical arms of paired sternopleural bridges close to each other, bullar lobes not visible (Fig. 2B, D).

Antennule: internal ventral border of basal article with sharp spine in middle portion (Fig. 2A).

Antenna: reaching posterior margin of carapace when extended back. Antennal scale widest at distal to mid-length, reaching middle of third antennal article, ASW 36.6% of ASL (Fig. 2A, C), lateral margin straight, distal spine well developed. Coxa with weakly prominent carina above nephropore. Basis unarmed (Fig. 2A).

Mandible: cephalic molar process molariform, caudal molar process bicuspidate with 1 cephalodistal cusp and 1 distoproximal cusp. Incisor lobe with 10 teeth; third tooth from anterior margin being largest (Fig. 2E).

Third maxilliped: ischium, ventral surface covered by tufts of composite setae with some sparse long and simple setae (Fig. 2F); dorsal surface with few setiferous punctations on inner margin and dorsal surface and 2 short, serrated setae on proximal portion (Fig. 2G); 'crista dentata' bearing 23 teeth on both right and left ischia (Fig. 2F, G). Merus, dorsal surface glabrous in proximal and middle portions, anterior outer margin portion with few long, serrated setae. Merus ventral surface sparsely covered by some long simple setae in median and outer regions (Fig. 2F); exopod longer than ischium, with flagellum surpassing proximal margin of merus and with tufts of long and composite setae in last and first articles (Fig. 2F, G).

First pair of pereiopods (chelipeds): large and subequal, laterally flattened (RPrT 25.3% of RPrL; LPrT 23.9% of LPrL) (Figs. 1A; 2I). Ischium ventral surface with 6 and 4 tubercles in right and left, respectively. Merus: right merus (RML) 60.2% of propodus length (RPrL); left merus (LML) 59.4% of propodus length (LPrL); ventral surface with 2 longitudinal series of tubercles: inner series with 17 tubercles, outer 11, plus 15 mesial tubercles irregularly distributed on right merus; inner series with 11 tubercles, outer 12, plus 14 mesial tubercles irregularly distributed on left merus. Dorsal and midventral spines absent. Carpus with dorsomedial surface not divided longitudinally by groove (Figs. 1A; 2I). Internal dorsolateral margin with row of tubercles, increasing in size distally; inner surface with 20 small mesial tubercles. Carpal spine absent (Fig. 2I). Propodus width (RPrW and LPrW) 46.3% of length in right cheliped and 45.5% in left cheliped. Dorsal surface of palm with irregularly distributed rows of squamous tubercles (Fig. 2H, I). Inner margin without tubercles. Ventral surface bearing 2 rows of squamous tubercles, surpassing the proximal part of fixed finger (Fig. 2H). Dactylus: articulating sub-vertically, right dactylus long (RDL) 69.4% of propodus length (RPrL), left dactylus long (LDL) 71.2% of left propodus (LPrL); dorsal surface with few squamous tubercles more concentrated in proximal portion (Fig. 2H). Cutting edge of fingers visible. Fixed finger with 10 teeth, fifth tooth largest in right cheliped. Dactyli with 12 teeth, third tooth largest in both chelipeds (Fig. 2H, I); right fixed finger with 11 teeth, left fixed finger with 9 teeth; fifth tooth largest. Second pair of pereiopods: dorsal surface of dactylus and propodus with tufts of long and simple setae. Dorsal and ventral surface of carpus with few sparse, simple and long setae in (Fig. 2J).

Gonopores: presence of both genital apertures on coxae of third and fifth pairs of pereiopods. Female gonopores semi-ellipsoidal (maximum diameter 1.35 mm) with well-calcified membrane. Male gonopores rounded, opening onto apical end of small, fixed, calcified and truncated phallic papilla, close to inner border of ventral surface of coxae of fifth pair of pereiopods. Male cuticle partition present (Fig. 2B).

Branchial count: 20 + epr + r. Branchial arrangement follows the same described by Hobbs (1991) with epipod of first maxilliped with rudimentary podobranchial filaments.

Measurements: holotype male, CL 31.8 mm and TL 61.1 mm. In the type series, CL ranges from 27.8 to 31.8 mm (mean = 29.8 mm). FW/CW: 0.43 ± 0.12 (min: 0.29; max: 0.53). RL/RW: 0.82 ± 0.06 (min: 0.76; max: 0.87). CMW/OW: 0.75 ± 0.08 (min: 0.70; max: 0.85). Postorbital carina longer than the rostral carina in all specimens analyzed. CW/PW: 1.05 ± 0.05 (min: 1.02; max: 1.09). AreW/RW: 0.71 ± 0.11 (min: 0.64; max: 0.79) (Tab. 1).

Color of living specimens. Data not available.

Table 1. Measurements (mm) of the type series of *Parastacus longidactylus* sp. n.. For abbreviations, see Material and Methods.

	Holotype male (MZUSP 45071)	Paratype female (MZUSP 45072)	Paratype male (MZUSP 45073)
TL	61.10	55.90	–
CL	31.80	27.80	–
CW	11.40	12.05	13.20
CD	13.50	14.00	16.80
CeL	21.10	18.30	22.90
RL	3.70	3.10	3.20
RW	4.40	3.55	4.20
RCL	7.80	4.60	6.40
CMW	1.26	1.30	1.25
OW	1.49	1.85	1.74
POCL	8.10	5.90	8.20
FW	6.12	3.55	5.70
ASL	4.40	3.33	3.55
ASW	1.60	1.25	1.70
AreL	8.80	7.90	–
AreW	2.80	2.80	–
LPrT	5.30	2.20	4.10
LPrL	22.20	9.10	19.20
LPrW	10.10	3.10	8.90
LDL	15.80	6.20	14.10
LML	13.20	6.70	13.80
RPrT	5.80	5.20	8.00
RPrL	22.90	–	25.10
RPrW	10.60	9.00	12.00
RDL	15.90	12.10	15.70
RML	13.80	10.90	13.70
PL	23.20	21.10	–
PW	11.20	11.05	–
TeL	9.10	8.70	10.40
TeW	7.30	6.80	8.20

Variations in type-series. All paratypes exhibit both masculine and feminine gonopores in the same individual. Male paratypes also exhibit semi-ellipsoidal female gonopores (average maximum diameter 1.36 mm) covered by a calcified membrane. Male gonopores are very similar in all male paratypes. The number of teeth in the 'crista dentata' ranges from 20 to 25 in the left ischium and from 19 to 26 in the right ischium of the third maxilliped in the paratypes.

Distribution. *Parastacus longidactylus* sp. n. appears to have a limited distribution, being registered so far only from the municipality of Amaral Ferrador, state of Rio Grande do Sul, southern Brazil (Fig. 4).

Habitat and Ecology. *Parastacus longidactylus* sp. n. was collected in the "Ladrão" creek near to the junction with the Camaquã River, in the Camaquã hydrographic basin, in the state of Rio Grande do Sul (Fig. 4). It is also part of the physiographic region of Serra do Sudeste region, bordering the Encosta do Sudeste region (IBGE 2004a; 2004b; UFRGS-IB-Centro de Ecologia, 2016).

Vegetation. The type locality of this species is in the Pampa biome. Types of vegetation in the area are Submontane Semideciduous Seasonal Forest, and Alluvial Semideciduous Seasonal Forest, commonly called gallery forest, or riparian forest, in the lower part, flat and prone to flooding in the rainy season (Beier *et al*., 2018; Rambo, 2015; SEMA, 2023).

Soil. The soil is classified as Dystrophic Red-Yellow Argisols (Santos *et al*., 2011). This soil usually occurs in areas of undulating relief, yet they may also be present in less steep areas. It has a characteristic yellowish-red color, which is related to higher levels of hematite and goethite iron oxides (Santos *et al*., 2023). Moreover, they are considered deep soils, with high drainage capacity, low fertility, nutrient limitations, strong acidity, and high susceptibility to degradation and erosion (Santos *et al*., 2011; 2023; Streck *et al*., 2002; 2008).

Burrowing behavior and burrow structure. Data not available.

Conservation status. Data Deficient. The extent of occurrence (EOO) was estimated as comprising approximately 6,968 km^2 (B1) (Fig. 4). Considering the data concerning the Camaquã River Hydrographic Basin, this species can only be classified under subitem b(iii): continuing decline observed in quality of habitat (IUCN, 2019). Taking this into account, we classified this species as DATA DEFICIENT (DD).

DISCUSSION

Morphology

Parastacus longidactylus sp. n. differs from *P. brasiliensis*, *P. buckupi*, *P. guapo*, *P. gomesae*, *P. macanudo*, and *P. promatensis* by the large eyes, rostral carina surpassing rostral basis and extending almost to the middle of postorbital carinae, cheliped palm dorsal surface with irregularly distributed verrucose tubercules, long dactylus, and blunt telson lateral spines (Figs. 1A–C, G; 2H, I; Tab. 2).

The present new species is morphologically similar to *P. brasiliensis* in regard to the general shape of rostrum and shape of the telson (sub-rectangular) (Fig. 1A–C, G; Tab. 2). It differs from *P. brasiliensis* in the straight rostral surface, prominent postorbital carinae, hexagonal anteromedian lobe of the epistome, mandible incisor process with ten teeth, narrow areola, and short pleon (Figs. 1A–C; 2A, E; Tab. 2).

It is also morphologically similar to *P. buckupi* in the general shape of the rostrum, and in the shape of the telson (subrectangular) (Fig. 1A–C, G; Tab. 2); it differs from *P. buckupi* in the straight and blunt rostral spine, prominent postorbital carinae, hexagonal anteromedian lobe of the epistome, bicuspidate mandible caudal molar process, and flattened chelipeds (Figs. 1A–C; 2A, E, I; Tab. 2).

The long-finger crayfish is morphologically similar to *P. gomesae* in the general shape of the rostrum, and in the shape of the telson (subrectangular) (Fig. 1A–C, G; Tab. 2); it differs from *P. gomesae* in the straight and blunt rostral spine, straight rostral surface, suborbital angle = 90°, prominent postorbital carina, mandible incisor process with ten teeth (the third tooth from the anterior margin is the largest), and smooth cheliped palm internal surface (Figs. 1A–C; 2E; Tab. 2).

Parastacus longidactylus sp. n. is morphologically similar to *P. guapo* in the general shape of the rostrum, and in the shape of the telson (subrectangular) (Fig. 1A–C, G; Tab. 2); it differs from *P. guapo* in the straight and blunt rostral spine, suborbital angle = 90°, prominent postorbital carina, hexagonal anteromedian lobe of the epistome, mandible incisor process with ten teeth, absent carpal spine, and smooth cheliped palm internal surface (Figs. 1A–C; 2A, E, H, I; Tab. 2).

Additionally, *P. longidactylus* sp. n. is morphologically similar to *P. macanudo* in the general shape of the rostrum, and in the shape of the telson (subrectangular) (Fig. 1A–C, G; Tab. 2); it differs from *P. macanudo* in the suborbital angle = 90°, prominent postorbital carina, hexagonal anteromedian lobe of the epistome, mandible incisor process with ten teeth (the third tooth from the anterior margin is the largest), absent carpal spine and short pleon (Figs. 1A, C; 2A, E, I; Tab. 2).

Finally, *P. longidactylus* sp. n. is morphologically similar to *P. promatensis* in the general shape of the rostrum, and in the shape of the telson (subrectangular) (Fig. 1A–C, G; Tab. 2); it differs from *P. promatensis* in the rounded rostrum apex (ending in a straight blunt spine), straight rostrum dorsal surface, cervical groove weakly V-shaped, hexagonal anteromedian lobe of the epistome, mandible incisor process with ten teeth, smooth cheliped palm internal surface, and short pleon (Figs. 1A–C; 2A, E; Tab. 2).

Table 2. Main characters distinguishing *Parastacus longidactylus* sp. n. from other species of *Parastacus* cited in the Remarks. Asterisk (*) indicates variations in species of comparative material. For abbreviations, see Material and Methods.

Characters		*P. brasiliensis*	*P. buckupi*	*P. gomesae*	*P. guapo*	*P. longidactylus* sp. n.	*P. macanudo*	*P. promatensis*
Rostrum								
	Shape	Triangular or spatulated	Triangular	Triangular	Triangular	Triangular	Triangular	Subtriangular
	Apex	Rounded, ending in an upward spine	Rounded, ending in an upward spine	Rounded and smooth*	Rounded, ending in an upward spine	Rounded, ending in a straight blunt spine	Rounded, ending in a tiny straight blunt spine*	Acute, ending in a short and depressed spine.
	Dorsal Surface	Concave	Straight	Straight with a slightly concave in the anterior portion	Straight	Straight	Straight	Flat
	Eyes	Small	Small	Small*	Small	Large	Small	Small
	Rostral carina	Surpassing the rostral basis	Surpassing the rostral basis	Surpassing the rostral basis	Surpassing the rostral basis	Surpassing rostral basis and extending almost to the middle of postorbital carinae	Surpassing the rostral basis	Surpassing the rostral basis
Suborbital angle		=90°	=90°	>90° *	>90°*	=90°	>90°	=90°
Postorbital carina		Weakly prominent	Weakly prominent	Prominent in anterior and middle portions	Prominent in anterior and middle portions	Prominent	Weakly prominent	Prominent
Cervical groove		Weakly V-shaped	Weakly V-shaped	Weakly V-shaped	Weakly V-shaped	Weakly V-shaped	Weakly V-shaped	U-shaped
Epistome								
	Anteromedian lobe	Pentagonal	Pentagonal	Septagonal	Pentagonal	Septagonal	Pentagonal	Pentagonal
Mandible								
	Incisor process	Nine teeth (the third tooth from the anterior margin is the largest)	Ten teeth (the fourth tooth from the anterior margin is the largest)	Seven teeth (the second tooth from the anterior margin is the largest)	Nine teeth (the third tooth from the anterior margin is the largest)*	Ten teeth (the third tooth from the anterior margin is the largest)	Nine teeth (the second tooth from the anterior margin is the largest)	Nine teeth (the third tooth from the anterior margin is the largest)
	Caudal molar process	Bicuspidate	Unicuspidate	Bicuspidate	Bicuspidate	Bicuspidate	Bicuspidate	Bicuspidate

Table 2. Cont.

Characters		*P. brasiliensis*	*P. buckupi*	*P. gomesae*	*P. guapo*	*P. longidactylus sp. n.*	*P. macanudo*	*P. promatensis*
Chelipeds								
	Carpal spine	Absent	Absent	Absent	Present	Absent	Present	Absent
	Size and shape	Large and flattened	Large and globose	Large and flattened	Large and flattened	Large and flattened	Large and flattened	Large and flattened
	Palm dorsal surface	2-3 rows of verrucose tubercles irregularly distributed	2 rows of verrucose tubercles irregularly distributed	3-4 rows of verrucose tubercles irregularly distributed	2-3 rows of verrucose tubercles irregularly distributed	Verrucose tubercles irregularly distributed	Single row of verrucose tubercles irregularly distributed	3-4 rows of verrucose tubercles irregularly distributed
	Palm internal surface	Smooth	Smooth	Few small tubercles	Sparse tubercles more concentrated in the low portion and close to the insertion of dactylus	Smooth	Smooth	Tubercles in medial portion
	Dactylus Size	Medium	Medium	Short	Medium	Long	Medium	Medium
Areola		Wide	Narrow	Narrow	Narrow*	Narrow	Narrow	Narrow
Pleon								
	Shape	Long and wide	Short and wide	Short and wide*	Short and wide*	Short and wide	Long and wide	Long and wide
Telson								
	Shape	Subrectangular	Subrectangular	Subrectangular	Subrectangular	Subrectangular	Subrectangular	Subrectangular
	Lateral spines	Large and sharp	Small and sharp	Small and sharp	Large and sharp	Small and blunt	Large and sharp	Large and sharp
References		Buckup and Rossi (1980); Miranda *et al.* (2018); Ribeiro *et al.* (2020).	Huber *et al.* (2018); Ribeiro *et al.* (2020).	Huber *et al.* (2022).	Huber *et al.* (2022).	Present paper.	Huber *et al.* (2020); Ribeiro *et al.* (2020).	Fontoura and Conter (2008); Miranda *et al.* (2018); Ribeiro *et al.* (2020).

Conservation status

Assessing the conservation status of a newly described species can be problematic due to the lack of knowledge of the general biology, population demographics, and distribution (Boos *et al.*, 2019). This situation is common with aquatic invertebrate fauna since their conservation status is usually rated using criterion B from IUCN. This criterion takes into consideration the decline in the habitat quality, the geographic distribution of the species and the fragmentation of its population (Cumberlidge *et al.*, 2009; 2017; Ribeiro *et al.*, 2016; 2017; Santos *et al.*, 2017; Huber *et al.*, 2018; 2020; 2022; Miranda *et al.* 2018; IUCN, 2019). In this contribution, to estimate the distribution of *P. longidactylus* sp. n., we calculated its EOO. According to the IUCN (2019), an EOO between 5,000 and 20,000 km^2, added to at least two conditions or subitems of this criterion, categorizes a species as Vulnerable (VU). However, *Parastacus longidactylus* sp. n. can only have subitem b(iii) apply, related to the observed decline in the quality of habitat due to local threats, which is the case in the Camaquã River Hydrographic Basin (CRHB) region (Fig. 4).

The CRHB has been suffering modification of its natural characteristics due to human occupation and activities, such as the replacement of native vegetation by crops and livestock, water pollution (disposal of agricultural pesticides and organic material, domestic sewage, and solid waste) and soil erosion (Lima and Silva, 2013; SEMA, 2015; Lense *et al.*, 2022). The main crops in the CRHB are rice plantations and forestry of *Eucalyptus* spp, "Acácia Negra" (*Acacia mearnsii*) and pine (*Pinus elliottii*), which are considered invasive species and can affect the surrounding natural environments (Beier *et al.*, 2018; SEMA, 2015). These crops represent a serious risk to the natural environment since usually they are irrigated using channels from natural water bodies, which causes a reduction in the volume of these natural water bodies, contamination by pesticides, soil compaction, fragmentation, and erosion (SEMA, 2015; Lense *et al.*, 2022). Furthermore, the region also suffers from deforestation and fragmentation of riparian forests, which increases erosion of the banks, while also causing significant loss of forested soil and increased siltation of the water bodies (De Marchi, 2006; Borges-Martins *et al.*, 2007; Didoné *et al.*, 2014; Chen *et al.*, 2019).

In conclusion, even with literature data for the CRHB region and the estimated EOO of *P. longidactylus* sp. n., it is still difficult to infer how limited and fragmented the distribution and population of this species are. Based on that, we suggest that *P. longidactylus* sp. n. should be categorized as Data Deficient (DD) for now. However, we reinforce the necessity of exploring the CRHB area to check for new records of this species, and evaluate its real distribution, habitat conservation, and population connectivity.

Updated key to genus Parastacus.

The following key is modified from Huber *et al.* (2022), with the addition of *Parastacus longidactylus* sp. n.

1 Telson with lateral spines 2

1' Telson without lateral spines, maxilliped III exopod flagellum surpassing ischium distal margin .... *Parastacus nicoleti* (Philippi, 1882)

2(1) Postorbital carina proximal edge ending in a strong spine; uropod protopod proximal lobe bearing a spine; areola delimited by carinae 3

2' Postorbital carina proximal edge not ending in spine; uropod protopod lobe lacking spine; areola not delimited by carinae 4

3(2) Cheliped merus, carpus, and propodus medially with tufts of long setae; maxilliped III ischium ventral margin with longitudinal spine row .... *Parastacus varicosus* Faxon, 1898

3' Cheliped merus, carpus, and propodus medially glabrous; maxilliped III ischium ventral margin with longitudinal tubercle row .... *Parastacus saffordi* Faxon, 1898

4(2') Telson distal margin rounded.. 5
4' Telson distal margin acute .... *Parastacus buckupi* Huber, Ribeiro and Araujo, 2018

5(4) Cheliped carpus distally glabrous 6
5' Cheliped carpus distally with tufts of long and simple setae ....
.... *Parastacus pilicarpus* Huber, Ribeiro and Araujo, 2018

6(5) Epistome anteromedian lobe hexagonal or pentagonal 7
6' Epistome anteromedial lobe septagonal 8

7(6) Cheliped dactyl and pollex cutting edges covered by long setal tufts.. 9
7' Cheliped dactyl and pollex cutting edges visible 10

8(6') Dactylus long .... *Parastacus longidactylus* sp. n.
8' Dactylus short .... *Parastacus gomesae* Huber, Araujo and Ribeiro, 2022

9(7) Postorbital carinae prominent .... *Parastacus pilimanus* (von Martens, 1869)
9' Postorbital carinae obsolete .... *Parastacus laevigatus* Buckup and Rossi, 1980

10(7') Chelipeds with globose palm 11
10' Chelipeds with flattened palm 13

11(10) Cervical groove U-shaped .... *Parastacus caeruleodactylus* Ribeiro and Araujo in Ribeiro *et al*., 2016
11' Cervical groove V-shaped 12

12(11') Rostral carinae reaching postorbital carinae proximal edge .... *Parastacus defossus* Faxon, 1898
12' Rostral carinae surpassing postorbital carinae proximal edge ... *Parastacus pugnax* (Poeppig, 1835)

13(10') Telson subrectangular 14
13' Telson subtriangular .... *Parastacus fluviatilis* Ribeiro and Buckup in Ribeiro *et al*., 2016

14(13) Cheliped palm dorsal surface with tubercles irregularly distributed 15
14' Cheliped palm dorsal surface with three well-defined tubercle rows ....
.... *Parastacus tuerkayi* Ribeiro, Huber and Araujo in Ribeiro *et al*., 2017
15(14) Cheliped ventral surface bearing one row of squamose tubercles 17
15' Cheliped ventral surface bearing two rows of squamose tubercles 16

16(15') Postorbital carinae prominent in anterior and middle portions ....
.... *Parastacus guapo* Huber, Araujo and Ribeiro, 2022
16' Postorbital carinae weakly prominent..
....*Parastacus macanudo* Huber, Rockhill, Araujo and Ribeiro, 2020

17(15) Cheliped palm medial margin tuberculate, cervical groove U-shaped ....
.... *Parastacus promatensis* Fontoura and Conter, 2008
17' Cheliped palm medial margin smooth; groove weakly V-shaped ....
.... *Parastacus brasiliensis* (von Martens, 1869)

ACKNOWLEDGMENTS

We thank the anonymous reviewers for their suggestions.

REFERENCES

ANA – Agência Nacional de Águas Brasil 2007. Manual de construção de base hidrográfica ottocodificada: fase 1 - construção da base topológica de hidrografia e ottobacias conforme a codificação de bacias hidrográficas de Otto Pfafstetter: versão 2.0 de 1/11/2007. Brasília, Agência Nacional de Águas, Superintendência de Gestão da Informação, 141 p.

Beier VB; Poleto C and Ferreira MEMC 2018. Processos antrópicos e a caracterização do baixo curso do Rio Camaquã no município de Cristal-RS. IV Encontro Regional de Geografia e XXVI Semana de Geografia: Geotecnologias no Mercado de Trabalho do Geógrafo: 433–447. ISBN 978-85-87884-40-4. Available at https://lume.ufrgs.br/handle/10183/192962. Accessed on 03 January 2023.

Boos H; Salge PG and Pinheiro MAA 2019. Conservation status and threats of Aeglidae: beyond the assessment. p. 233–255. In: Santos S and Bueno SLS (Eds.) and Wehrtmann IS (Series Ed.), Aeglidae: Life History and Conservation Status of Unique Freshwater Anomuran Decapods. Advances in Crustacean Research, v. 21. New York: CRC - Taylor & Francis Group.

Borges-Martins M; Alves MLM; Araujo ML de; Oliveira RB de and Anés AC 2007. Áreas importantes para conservação na Planície Costeira do Rio Grande do Sul. In: Becker FG; Ramos RA and Moura LA (Orgs.), Biodiversidade: Regiões da Lagoa do Casamento e dos Butiazais de Tapes, Planície Costeira do Rio Grande do Sul. Brasília:,Ministério do Meio Ambiente, 385p.

Buckup L and Rossi A 1980. O gênero *Parastacus* no Brasil (Crustacea, Decapoda, Parastacidade). *Revista Brasileira de Biologia*, 40: 663–681.

Chen Z; Wang L; Wei A; Gao J; Lu Y and Zhou J 2019. Land-use change from arable lands to orchards reduced soil erosion and increased nutrient loss in a small catchment. *Science of The Total Environment*, 648: 1097–1104. https://doi.org/10.1016/j.scitotenv.2018.08.141

Crandall KA and Buhay JE 2008. Global diversity of crayfish (Astacidae, Cambaridae, and Parastacidae-Decapoda) in freshwater. *Hydrobiologia*, 595: 295–301. https://doi.org/10.1007/s10750-007-9120-3.

Cumberlidge N; Rasamy RJ; Ranaivoson CH; Randrianasolo HH; Sayer C; Máiz-Tomé L; Van Damme D and Darwall WRT 2017. Updated extinction risk assessments of Madagascar's freshwater decapod crustaceans reveal fewer threatened species but more Data Deficient species. *Malagasy nature*, 12: 32–41.

Cumberlidge N; Ng PKL; Yeo DCJ; Magalhães C; Campos MR; Alvarez F; Naruse T; Daniels SR; Esser LJ; Attipoe FYK; Clotilde-Ba FL; Darwall W; McIvor A; Baillie JEM; Collen B and Ram M 2009. Freshwater crabs and the biodiversity crisis: importance, threats, status, and conservation challenges. *Biological Conservation*, 142(8): 1665–1673. https://doi.org/10.1016/j.biocon.2009.02.038

De los Rios-Escalante PR; Jara-Seguel P; Contreras A; Latsague M; Lara G; Rudolph E and Crandall KA 2022. Distributional patterns of the South American species of Parastacidae (Decapoda, Astacidea). *Crustaceana*, 95(10-12): 1123–1136. https://doi.org/10.1163/15685403-bja10247.

De Marchi T 2006. Estudo do componente arbóreo de mata ribeirinha no rio Camaquã, Cristal, RS. Porto Alegre, Universidade Federal do Rio Grande do Sul, Master dissertation, 65p. [Unpublished]. Available at https://www.lume.ufrgs.br/handle/10183/7462. Accessed on 04 January 2023.

Didoné EJ; Minella JPG; Reichert JM; Merten GH; Dalbianco L; Barrros, CAP and Ramon R 2014. Impact of no-tillage agricultural systems on sediment yield in two large catchments in Southern Brazil. *Journal of Soils and Sediments*, 14: 1287–1297. https://doi.org/10.1007/s11368-013-0844-6

Faxon W 1898. Observations on the Astacidae in the United States National Museum and in the Museum of Comparative Zoology, with descriptions of new species. *Proceedings of the United States National Museum*, 20 (1136): 642–694. https://doi.org/10.5479/si.00963801.20-1136.643.

Fontoura NF and Conter MR 2008. Description of a new subspecies of the crayfish *Parastacus brasiliensis* (Von Martens, 1869) from São Francisco de Paula, RS, Brazil (Decapoda, Parastacidae). *Zootaxa*, 1849(1): 28–34. https://doi.org/10.11646/zootaxa.1849.1.2.

Hobbs HH Jr 1991. A new generic assignment for a South American crayfish (Decapoda, Parastacidae) with revised diagnoses of the South American genera and comments on the parastacid mandible. *Proceeding of the Biological Society of Washington*, 104(4): 800–811.

Horn ACM; Buckup L; Noro CK and Barcelos DF 2008. Morfologia externa de *Parastacus brasiliensis* (Decapoda, Parastacidae). *Iheringia,* Série Zoologia, 98 (1): 148–155. https://doi.org/10.1590/S0073-47212008000100019

Huber AF; Ribeiro FB and Araujo PB 2018. New endemic species of freshwater crayfish *Parastacus* Huxley, 1879 (Crustacea: Decapoda: Parastacidae) from the Atlantic forest in southern Brazil. *Nauplius*, 26: e2018015. https://doi.org/10.1590/2358-2936e2018015

Huber AF; Araujo PB and Ribeiro FB 2022. The hole is deeper: description of two new species within the *Parastacus brasiliensis* (von Martens, 1869) species complex with an integrative taxonomy approach. *Zootaxa*, 5168 (3): 251–284. doi.org/10.11646/zootaxa.5168.3.1.

Huber AF; Rockhill ER; Araujo PB and Ribeiro FB 2020. A new species of burrowing crayfish in genus *Parastacus* Huxley, 1879 (Decapoda, Parastacidae) from the Sinos River Basin, Southern Brazil. *Zoological Studies*, 59 (47). https://doi.org/10.6620/ZS.2020.59-47

Huxley TH 1879. On the classification and the distribution of the crayfishes. *Proceedings of the Zoological Society of London*, 46(1): 752–788. https://doi.org/10.1111/j.1469-7998.1878.tb08020.x

IBGE—Instituto Brasileiro de Geografia e Estatística, Biomas e Sistema Costeiro-Marinho do Brasil 2004a.

Solos 1:5.000.000. Available at https://www.ibge.gov.br/geociencias/informacoes-ambientais/pedologia/15829-solos.html?=&t=o-que-e. Accessed on 02 January 2023.

IBGE – Instituto Brasileiro de Geografia e Estatística, Biomas e Sistema Costeiro-Marinho do Brasil 2004b. Vegetação Brasileira 1:5.000.000, Available at https://www.ibge.gov.br/geociencias/informacoes-ambientais/vegetacao/10872-vegetacao.html?=&t=o-que-e. Accessed 02 January 2023.

IUCN – International Union for Conservation of Nature 2019. Guidelines for Using the IUCN Red List Categories and Criteria. Version 14. Prepared by the Standards and Petitions Committee. Available at http://www.iucnredlist.org/documents/RedListGuidelines.pdf. Accessed on 02 January 2023.

Lense GHE; Baitelli R and Mincato RL 2022. Modelagem de perdas de solo na bacia hidrográfica do rio Camaquã, sul do Brasil. *Revista Brasileira de Ciências Agrárias*, 17(4): 1–7. https://doi.org/10.5039/agraria.v17i4a1521

Lima LB and Silva LFM 2013. Os principais problemas ambientais da bacia hidrográfica do rio Camaquã. *Anais Do Salão Internacional De Ensino, Pesquisa E Extensão*, 4(2). Available at https://periodicos.unipampa.edu.br/index.php/SIEPE/article/view/60127. Accessed on 04 January 2023.

Miranda I; Gomes KM; Ribeiro FB; Araujo PB; Souty-Grosset C and Schubart CD 2018. Molecular systematics reveals multiple lineages and cryptic speciation in the freshwater crayfish *Parastacus brasiliensis* (von Martens, 1869) (Crustacea: Decapoda: Parastacidae). *Invertebrates Systematics*, 32: 1265–1281. https://doi.org/ 10.1071/IS18012

Philippi RA 1882. Zoología chilena. Sobre los *Astacus*. *Anales de la Universidad de Chile*, 61: 624–628. https://doi.org/10.5354/0717-8883.2012.21621

Poepigg E 1835. Reise in Chile, Peru und auf dem Amazonas strome, während der Jahre. *Fleischer und Hinrichs*, Leipzig, 1: 1827–1832.

QGIS Development Team 2021. QGIS Geographic Information System. Open Source Geospatial Foundation Project. Available at http://qgis.osgeo.org. Accessed 02 January 2023.

Rambo BSJ 2015. A fisionomia do Rio Grande do Sul. 4ª edição revisada. São Leopoldo, Editora Unisinos, 398p.

Ribeiro FB; Buckup L; Gomes KM and Araujo PB 2016. Two new species of South American freshwater crayfish genus *Parastacus* Huxley, 1879 (Crustacea: Decapoda: Parastacidae). *Zootaxa*, 4158(3): 301–324. https://doi.org/10.11646/zootaxa.5158.3.1

Ribeiro FB; Huber AF; Schubart D and Araujo PB 2017. A new species of *Parastacus* Huxley, 1879 (Crustacea, Decapoda, Parastacidae) from a swamp forest in southern Brazil. *Nauplius*, 25: e2017008. https://doi.org/10.1590/2358-2936e2017008

Ribeiro FB; Gomes KM; Huber AF and Loureiro TG 2020. Diversity and Conservation Strategies of Freshwater Crayfish in South America: An Update. p. 1–42. In: Ribeiro FB (Ed), Crayfish: Evolution, Habitat and Conservation Strategies. New York, Nova Science Publishers,

Riek EF 1971. The freshwater crayfishes of South America. *Proceedings of the Biological Society of Washington*, 84: 129–136.

Rogers DC; Magalhães C; Peralta M; Ribeiro FB; Bond-Buckup G; Price WW; Guerrero-Kommritz J; Mantelatto FL; Bueno A; Camacho AI; González ER; Jara CG; Pedraza M; Pedraza-Lara C; Latorre ER and Santos S 2020. Chapter 23—Phylum Arthropoda: Crustacea: Malacostraca. p. 809–986. In: Rogers DC; Damborenea, C. and Thorp J (Org.), Thorp and Covich's Freshwater Invertebrates. Vol. 5. 4th edition. Academic Press, Boston, Massachusetts: https://doi.org/10.1016/B978-0-12-804225-0.00023-x

Rudolph EH 1997. Intersexualidad en el camarón excavador *Parastacus pugnax* (Poeppig, 1835) (Decapoda, Parastacidae). *Investigaciones marinas*, 25: 7–18. https://doi.org/10.4067/S0717-71781997002500002

Rudolph EH 2015. Current state of knowledge on *Virilastacus* species (Crustacea, Decapoda, Parastacidae). *Latin American Journal of Aquatic Research*, 43(5): 807–818. https://doi.org/10.3856/vol43-issue5-fulltext-1

Rudolph EH and Almeida A 2000. On the sexuality of South American Parastacidae (Crustacea, Decapoda). *Invertebrate Reproduction & Development*, 37(3): 249–257. https://doi.org/10.1080/07924259.2000.9652425

Santos HG; Zaroni MJ; Almeida EPC and AGEITEC – Agência Embrapa de Ciência e Tecnologia 2023. Argissolos Vermelho-Amarelos. Available at https://www.embrapa.br/en/agencia-de-informacao-tecnologica/tematicas/solos-tropicais/sibcs/chave-do-sibcs/argissolos/argissolos-vermelho-amarelos. Accessed on 02 January 2023.

Santos HG; Carvalho-Junior W; Dart RO; Aglio MLD; Sousa JS; Pares JG; Fontana A; Martins ALS and Oliveira AP 2011. O novo mapa de solos do Brasil: legenda atualizada. Embrapa Solos, Rio de Janeiro. Available at http://geoinfo.cnps.embrapa.br/layers/geonode%3Asolos_br5m_2011_lat_long_wgs84. Accessed on 02 January 2023.

Santos S; Bond-Buckup G; Gonçalves AS; Bartholomei-Santos ML; Buckup L and Jara CG 2017. Diversity and conservation status of *Aegla* spp. (Anomura, Aeglidae): an update. *Nauplius*, 25: e2017011. https://doi.org/10.1590/2358-2936e2017011

SEMA - Secretaria do Meio Ambiente e Infraestrutura. 2015. Diagnóstico da bacia do Rio Camaquã (RT3). Porto Alegre, Gama Engenharia e Recursos Hídricos, Secretaria do Meio Ambiente e Infraestrutura do Estado do Rio Grande do Sul, 674 pp.

SEMA - Secretaria de Meio Ambiente e Infraestrutura. 2023. L030 - Bacia Hidrográfica do Rio Camaquã. Available from: https://sema.rs.gov.br/l030-bh-rio-camaqua. Accessed on 03 January 2023.

Streck EV; Kämpf N; Dalmolim RSD; Klamt E; Nascimento PC and Schneider P 2002. Solos do Rio Grande do Sul. UFRGS, Porto Alegre, 107p.

Streck EV; Kämpf N; Dalmolim RSD; Klamt E; Nascimento PC; Scheneider P; Giasson E and Pinto LFS 2008. Solos do Rio Grande do Sul. 2ª edition. EMATER/RS, Porto Alegre, 222p.

Toon A; Pérez-Losada M; Schweitzer CE; Feldmann RM; Carlson M and Crandall K 2010. Gondwanan radiation of the Southern Hemisphere crayfishes (Decapoda: Parastacidae): evidence from fossils and molecules. *Journal of Biogeography*, 37: 2275–2290. https://doi.org/10.1111/j.1365-2699.2010.02374.x

UFRGS-IB-Centro de Ecologia 2016. Mapeamento da cobertura vegetal do Bioma Pampa: Ano-base. Porto Alegre: UFRGSIB-Centro de Ecologia. Available at https://www.ufrgs.br/labgeo/index.php/dados-espaciais/245-mapeamento-dacobertura-vegetal-do-bioma-pampa-ano-base-2009. Accessed on 02 January 2023.

von Martens E 1869. Südbrasilische Süss- und Brackwasser-Crustaceen nach den Sammlungen des Dr. Reinh. Hensel. *Archiv für naturgeschichte*, 35: 1–37.

ADDITIONAL INFORMATION AND DECLARATIONS

Author Contributions

Conceptualization and Design: AFH, PBA, FBR. Performed research: AFH, PBA, FBR. Acquisition of data: AFH, PBA, FBR. Analysis and interpretation of data: AFH, PBA, FBR. Preparation of figures/tables/maps: AFH. Writing - original draft: AFH, PBA, FBR. Writing - critical review & editing: AFH, PBA, FBR.

Consent for publication

All authors declare that they have reviewed the content of the manuscript and gave their consent to submit the document.

Competing interests

The author(s) declare(s) no competing interest.

Data availability

All study data are included in the article.

Funding and grant disclosures

The Coordenação de Aperfeiçoamento de Pessoal de Nível Superior (CAPES) provided a Master's scholarship to A.F. Huber and a postdoctoral fellowship to F.B. Ribeiro (PNPD nr 88887.470134/2019-00).

Study permits

All sampled specimens were collected according to Brazilian laws (SISBIO license number 45759-5).